Can. J. Remote Sensing, Vol. 37, No. 5, pp. 1–9, 2011

Evaluation of the quad-polarimetric Radarsat-2 observations for the wetland InSAR application

Sang-Hoon Hong and Shimon Wdowinski

Abstract. Wetland interferometric synthetic aperture radar (InSAR) has been successfully applied to observe phase variations related to water level changes in aquatic environments with emergent vegetation. In this study, we evaluate the quadrant polarimetric Radarsat-2 (C-band) observations for the wetland InSAR applications by testing two datasets acquired over south Florida's Everglades wetlands. The first set was acquired over our northern study area, consisting of mostly managed wetlands and agricultural environments. The second set was acquired over our southern study area, consisting of naturally flowing fresh- and salt-water wetlands in the southern Everglades. In both sets, observations were acquired every repeat orbit (24 days) to generate interferograms with short temporal baselines that can maintain high coherence levels. Our results showed high coherence values in all polarization modes (from 0.26 to 0.42), with highest values in HH, then VV, and lowest in HV or VH. Surprisingly, all the quadrant polarimetric interferograms showed very similar fringe patterns regardless of the polarization type, suggesting that water level changes can be detected in all polarizations. Furthermore, the observations implied that double bounce is the dominant scattering mechanism, even in cross polarization (HV and VH), and not volume scattering as commonly assumed.

Résumé. L'interférométrie radar à synthèse d'ouverture (InSAR) en milieux humides a été appliquée avec succès à l'observation des variations de phases reliées aux changements du niveau de l'eau dans les environnements aquatiques caractérisés par de la végétation émergente. Dans cette étude, on évalue les observations des quadrants de données polarimétriques de Radarsat-2 (en bande C) pour des applications de données InSAR en milieux humides en testant deux ensembles de données acquis au-dessus des milieux humides des Everglades, dans le sud de la Floride. Le premier ensemble a été acquis au-dessus de notre site d'étude situé au nord qui consiste surtout en milieux humides aménagés et en zones agricoles. Le deuxième ensemble a été acquis au-dessus de notre site d'étude situé au sud qui consiste en milieux humides naturellement drainés par de l'eau douce et de l'eau salée dans le sud des Everglades. Pour les deux ensembles, les observations ont été acquises à chaque nouveau passage satellite (24 jours) afin de générer des interférogrammes avec des périodes temporelles courtes qui peuvent assurer des niveaux élevés de cohérence. Nos résultats montrent des valeurs élevées de cohérence pour tous les modes de polarisation (de 0,26 à 0,42), avec les valeurs les plus élevées en polarisation HH, puis VV et les plus faibles, en polarisation HV ou VH. Étonnamment, tous les interférogrammes polarimétriques montrent des patrons très semblables en bordure, indépendamment du type de polarisation, suggérant que les changements du niveau de l'eau peuvent être détectés dans toutes les polarisations. De plus, les observations démontrent que le double rebond est le mécanisme de diffusion dominant, même en polarisation croisée (HV et VH), et non la diffusion volumétrique comme généralement acquis.
[Traduit par la Rédaction]

Introduction

Wetland Interferometric Aperture Radar (InSAR) is a unique application of the InSAR technology that measures elevation changes of aquatic surfaces; all other InSAR applications measure changes of solid surfaces. It provides a high spatial resolution map of hydrological observations over the wetland that cannot be obtained by any terrestrial-based method. It works only in aquatic environments with emerged vegetation, as the combination of horizontal water surfaces with vertical vegetation provides efficient geometry for double-bounce scattering (Alsdorf et al., 2000; Wdowinski et al., 2004). The dependency of the wetland InSAR application on the vegetation enables us to use SAR phase measurements to better understand vegetation scattering, which is often evaluated only from SAR amplitude measurements.

Wetland InSAR was found to work successfully with all three radar wavelength signals (X-, C-, and L-band) as long as the time span between the observations (temporal baseline) is short (Wdowinski et al., 2004; Wdowinski et al., 2008; Gondwe et al., 2010; Hong et al., 2010a, 2010b). These are surprising results as the short and intermediate wavelength signals are assumed to interact with upper sections of the vegetation, as canopies and branches and, hence, should

Received 2 February 2011. Accepted 21 November 2011. Published on the Web at http://pubs.casi.ca/journal/cjrs on xxx xxx xxx.

Sang-Hoon Hong[1]. Satellite Data Application Department, Korea Aerospace Research Institute, Daejeon, 305-333, Korea.

Shimon Wdowinski. Division of Marine Geology and Geophysics, University of Miami, Miami, Florida, 33149-1098, USA.

[1]Corresponding Author (e-mail: shong@kari.re.kr).

not reflect surface changes. Another surprising result was the discovery that cross-polarization interferograms (HV and VH) also measure surface water level changes (Hong et al., 2010a), because most vegetation scattering theories assume that cross-polarization observations result only from volume scattering (Freeman and Durden, 1998; Yamaguchi et al., 2005).

In this study, we explore the feasibility of Radarsat-2 C-band quad-polarimetric data for the wetland InSAR application. The quad-polarization data enable us to better understand previous dual-polarization TerraSAR-X observations indicating the ability of cross-polarization data to detect water level changes (Hong et al., 2010a). Using a rigorous coherence analysis we evaluated the importance of key acquisition parameters, including polarization, temporal baseline, and perpendicular baseline, as well as vegetation type on the suitability of Radarsat-2 observation to the wetland InSAR application.

Study area

The Everglades, which are subtropical wetlands located in south Florida, have a large watershed characterized by a very wide, shallow, and slow sheetflow. The natural sheetflow includes the Kissimmee River, Lake Okeechobee, and the Everglades region (**Figure 1a**). In the past half century, construction of drainage canals and flood preventing levees disrupted the natural water flow and transformed a significant part of the wetland into agricultural and urban areas. The present-day Everglades wetlands comprise only about a third of the south section of the natural system. It consists of managed wetlands in the northern section, where the flow is controlled by a series of structures such as levees or gates, and naturally flowing wetlands in the southern section, which preserve the original wetland sheetflow. The water conditions in the Everglades wetlands are monitored by more than 200 stage stations, which is probably the densest stage network in the world; a significant part of the network was constructed to aid a restoration plan of Everglades. Thus, the Everglades wetlands provide an excellent testbed for evaluating hydrological related space-based observations.

In this paper, we focused on two areas with different characteristics. The northern study area is located at the eastern part of the managed wetlands (**Figure 1c**). The Radarsat-2 frame covers Water Conservation Areas (WCA) 1 and 2A, which are wetlands divided by a series of levees and serve as water storage for the southeast Florida population. The WCA areas are dominated mainly by sawgrass, a portion of wet prairies, and tree islands. The overall sheetflow pattern is a north–south flow; the water drains from WCA1 in the north and releases into WCA2A in the south. The hydrodynamics of the WCA areas are relatively simple compared with a natural wetland environment, because the flow in these areas is controlled

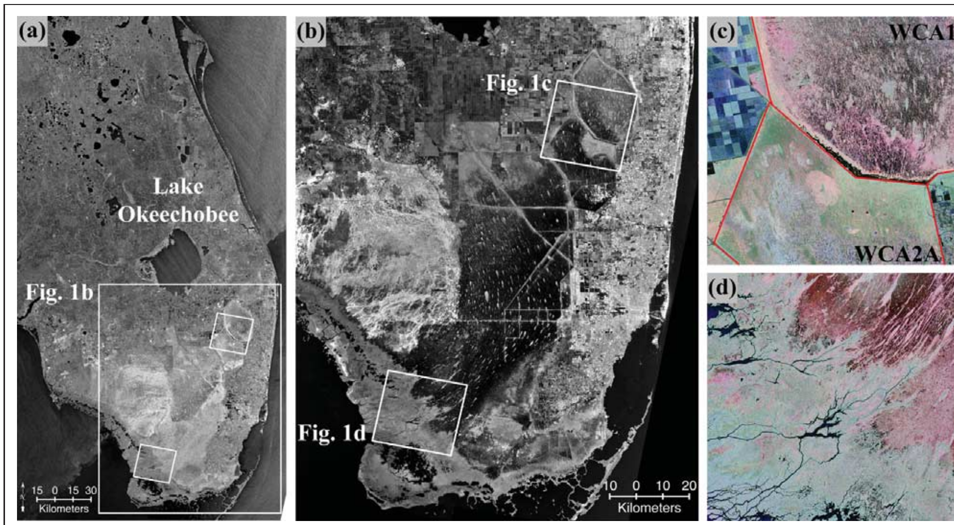

Figure 1. SAR amplitude images showing the study area in south Florida. (a) Radarsat-1 ScanSAR image of Florida showing location of study area (Radarsat data © Canadian Space Agency/Agence spatiale canadienne 2002. Processed by CSTARS and distributed by Radarsat International). (b) JERS-1 L-band amplitude image of south Florida showing the location map of the Radarsat-2 swathes. (c) Pauli decomposition of the Radarsat-2 amplitude data of the northern study area consisting of both wetland and agricultural environments; red, HH – VV (even scattering); green, HV (rotated dihedral); and blue, HH + VV (odd scattering). The red lines are hydrological structures surrounding the WCA1 and WCA2 areas. (d) Pauli decomposition of the Radarsat-2 amplitude data of the southern study area consisting of saltwater (mangrove) and freshwater wetlands; red, HH – VV (even scattering); green, – HV (rotated dihedral); and blue, – HH + VV (odd scattering).

by levees, gates, and other manmade structures. This area has been selected previously as a good test site to evaluate wetland InSAR techniques (Wdowinski et al., 2004; Wdowinski et al., 2006; Hong et al., 2010a, 2010b;).

The other study area is located in the southwestern part of the Everglades wetlands. This area is located within the Everglades National Park (ENP) comprising different types of wetland environments across the transition between freshwater and saltwater wetlands (**Figure 1d**). The northeastern part of the Radarsat-2 swath is covered with freshwater herbaceous vegetation, whereas the southwestern section is covered by saltwater woody vegetation, i.e., mangroves. Water level changes in the saltwater mangrove area are induced by tidal movement, as previously observed with X- and L-band data (Wdowinski et al., 2008; Hong et al., 2010a).

Radarsat-2 data and processing

As part of the Science and Operational Applications Research (SOAR) project, we obtained a 10-acquisition quota for investigating the usefulness of Rasdarsat-2 for wetland research. We used our quota by ordering and acquiring Radarsat-2 fine resolution beam quad-polarization (FQ) mode data over the two study areas, each characterized by a different wetland environment (**Table 1**). Because of the high acquisition resolution, the imagery area is limited to relatively small area of 25 km × 25 km (**Figure 1**). The technical details of the two datasets are described in **Table 2**.

We acquired seven scenes over the northern study area and three over the southern area. The first set consisted of seven consecutive acquisitions of the northern study area, with a 24 day repeat acquisition between 30 September 2008 and 21 February 2009. Temporal baseline ranged from 24 days to 144 days, the perpendicular baseline ranged from 5 m to 786 m, and stable Doppler centroid frequencies were found in all of datasets (the difference of Doppler centroid frequencies was less than only 50 Hz) (**Table 1**). These quad-polarimetric acquisitions enabled us to generate 21 quad-polarimetric interferograms (four polarimetric interferograms for each interferometric pairs). We acquired more scenes over the WCA1 of the northern study area because of the relative simplicity of the hydrodynamics and for the coherence analysis with a longer temporal baseline within the limited acquisition quota. The second set, which consisted of only three acquisitions with an 11 day repeat cycle, was collected over the southern study area, which is a natural wetland environment of ENP. The acquisition period was from 23 September 2008 to 17 October 2008 with 24–48 day temporal baselines and 88–502 m geometrical perpendicular baselines. This set allowed us to generate three quad-polarimetric interferograms.

Table 1. Radarsat-2 synthetic aperture radar data characteristics.

Parameter	Radarsat-2
Carrier frequency	5.405 GHz
Wavelength	5.55 cm
Polarization	Quad-pol
Repeat period	24 days
Beam mode	Fine Quad (F6/F10)
Flight direction	Descending
Incidence angle	26.2°/30.7°
Pulse repetition frequency	1421.96/1288.02 Hz
ADC sampling rate	31.67 MHz
Azimuth pixel spacing	4.70/5.18 m
Range pixel spacing	4.73/4.73 m

Table 2. List of Radarsat-2 C-band SAR interferometric pairs.

		SAR image			
Area	No.	Master	Slave	Absolute perpendicular baseline (m)	Temporal baseline (days)
WCA	1	2008-09-30	2008-10-24	125	24
WCA	2	2008-09-30	2008-11-17	250	48
WCA	3	2008-09-30	2008-12-11	5	72
WCA	4	2008-09-30	2009-01-04	194	96
WCA	5	2008-09-30	2009-01-28	592	120
WCA	6	2008-09-30	2009-02-21	191	144
WCA	7	2008-10-24	2008-11-17	376	24
WCA	8	2008-10-24	2008-12-11	130	48
WCA	9	2008-10-24	2009-01-04	69	72
WCA	10	2008-10-24	2009-01-28	717	96
WCA	11	2008-10-24	2009-02-21	317	120
WCA	12	2008-11-17	2008-12-11	246	24
WCA	13	2008-11-17	2009-01-04	445	48
WCA	14	2008-11-17	2009-01-28	341	72
WCA	15	2008-11-17	2009-02-21	59	96
WCA	16	2008-12-11	2009-01-04	199	24
WCA	17	2008-12-11	2009-01-28	587	48
WCA	18	2008-12-11	2009-02-21	187	72
WCA	19	2009-01-04	2009-01-28	786	24
WCA	20	2009-01-04	2009-02-21	385	48
WCA	21	2009-01-28	2009-02-21	400	24
ENP	1	2008-09-23	2008-10-17	414	24
ENP	2	2008-09-23	2008-11-10	88	48
ENP	3	2008-10-17	2008-11-10	502	24

Note: WCA, Water Conservation Areas (managed wetlands); ENP, Everglades National Park (naturally flowing wetlands).

Two Radarsat-2 datasets were processed with the ROI_PAC (Buckley et al., 2000) and Gamma software packages. These packages have the ability to calculate differential interferograms using digital elevation models (DEM) and eliminate topographic related phase changes. Before generating interferograms, all possible interferometric pairs were coregistered using amplitude correlation coefficients with master data from the very first acquisition in each dataset to compare interferograms. All possible interferograms, 96 in total, were generated in each polarimetric mode data. Most interferograms with short temporal baselines had sufficient interferometric coherence to observe the phase variations. The fringe patterns represent water level changes occurring between the two SAR acquisitions. The acquisition parameters such as temporal baseline, polarization, and

Vol. 37, No. 5, October/octobre 2011

surface conditions can affect the coherence level. Each dataset was coregistered at the same image coordinate to compare the quality of the interferograms. As part of the analysis, we removed topographic phase using the SRTM-1 DEM and applied interferometric filtering (Goldstein and Werner, 1998) to reduce speckle noises and to improve the signal to noise ratio of the interferograms. The small geometric, perpendicular, and stable Doppler centroid baselines were found at all interferometric pairs. Our results indicate that the Radarsat-2 satellite is well operated and its products are suitable for the wetland InSAR application.

Results

Managed wetland

We processed the 21 quad interferograms (total of 84 interferograms) using all possible interferometric pairs that were generated from the seven quad-polarization acquisitions. A quad interferogram contains four independent interferograms, one for each polarization. The quad-polarization interferogram presented in **Figure 2** shows a very similar fringe pattern in all four polarizations. It shows a discontinuous fringe pattern across hydrological structures, such as levees, reflecting independent water level changes in each of the WCAs. Overall, the coherent phases managed wetland with a short 24 day temporal baseline, because the radar signal can easily reach the sawgrass plain, which dominates the northern study area. Although the fringe pattern was very similar, the coherence level varied between the different polarizations. It was highest in the HH polarization, intermediate in the VV, and lowest in both cross-polarizations (HV and VH). The similar fringe pattern in all interferograms was a surprising result, as it opposed the expected behavior predicated by most vegetation scattering theories.

To investigate coherence variations due to temporal decorrelation, we present a series of interferograms with a

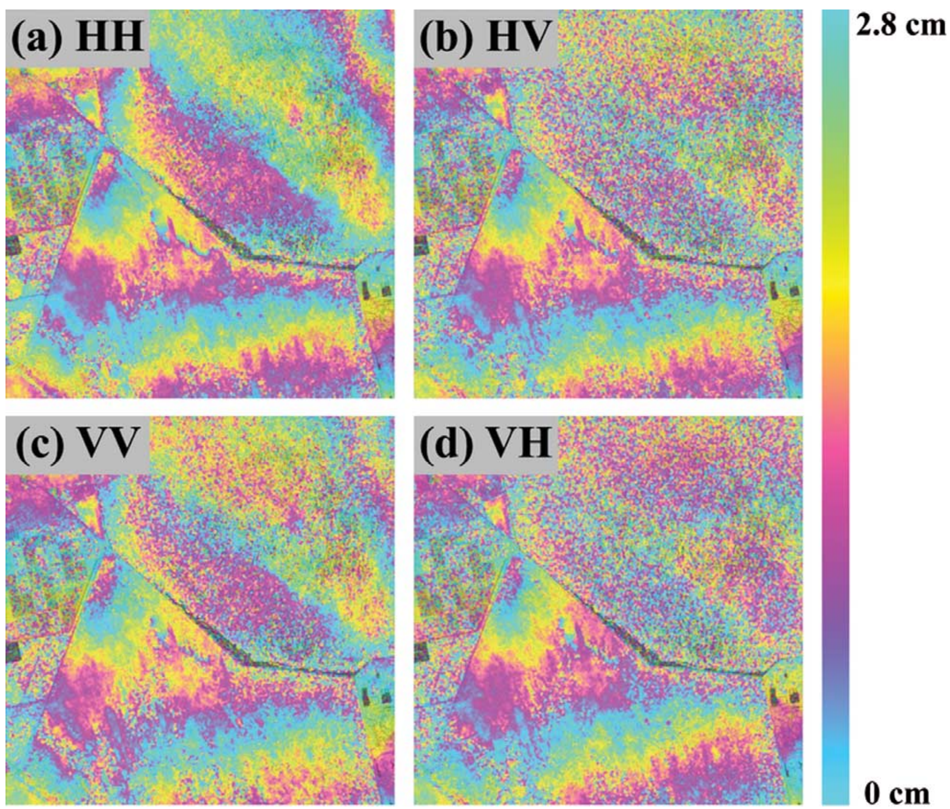

Figure 2. Radarsat-2 quad-polarimetric interferograms (28 January 2009 and 21 February 2009, Bperp: 448 m, temporal baselines (Btemp): 24 days) of wetlands in the northern study area. Each fringe cycle represents 2.8 cm change in the line of sight between the satellite and the surface. The fringe patterns in the wetlands show water level changes occurred between the two acquisitions. All interferograms show a similar fringe pattern reflecting water level changes in the wetlands. Discontinuous fringe patterns occur across levies separating the WCAs, due to independent water level changes in each area. The co-polarization interferograms (a and c) maintain higher coherence than the cross-polarization interferograms (b and d). The highest coherence level is found in the HH interferogram and lowest in both cross-polarization (HV and VH) interferograms.

24–144 day temporal baseline range (**Figure 3**). Our analysis showed that interferograms with a short temporal baseline (**Figures 3a** and **3b**) maintained high coherence levels in most wetland areas. Coherence was well maintained in the WCA-1 area in both the 24 and 48 day interferograms. However, only a partial coherence was detected in WCA-2A in the 48 day temporal baseline. Coherent phases were found only in the WCA-1 area with the longer time span interferograms (**Figures 3c**, **3d**, and **3e**). However, the 144-day interferogram had a little coherence over only the WCA1 area showing a coherent phase in the urban area (**Figure 3f**). The coherent phases were not detected in the agricultural area. We think that the incoherent phases were caused by seasonal changes after the harvesting of the agricultural area. Overall, coherence over the wetlands is better maintained in areas dominant by double-bounce scattering than in areas characterized by dominant volume scattering (**Figure 1c**).

We conducted a systematic coherence analysis of all possible interferograms by calculating interferometric coherence within a 5pixel $\times$ 5 pixel window (about 25 m^2 $\times$ 25 m^2) (**Figure 4**). Our results showed that the HH polarization maintained the best coherence (the maximum of about 0.4), and the VV coherence was higher than those of cross-polarizations (**Figure 4a**). The HH polarization data with a short temporal baseline, such as 24 days, maintained the greatest coherence compared with any other polarimetric data (**Figure 4b**). Our coherence study confirms previous results indicating that interferometric coherence in wetlands has inverse relations to temporal baseline (Wdowinski et al., 2006; Lu and Kwoun, 2008; Hong et al., 2010a). We plotted coherence in terms of temporal and geometrical perpendicular baselines (**Figure 5**). The coherence showed strong dependence on the temporal baseline and less dependence on the geometrical perpendicular baseline.

Natural wetland

We processed the three quad-interferograms using the three quad-polarization acquisitions of the southern study area. As in the northern study area, the quad interferograms showed a very similar fringe pattern in the four polarizations, but with variable coherence (**Figure 6**). The interferograms showed a low fringe gradient in the northeastern herbaceous area, which reflects water level change due to a north–south freshwater flow. A high fringe rate with short wavelength pattern was found in NW–SE belt at the central part of the interferogram. This area of high coherence was

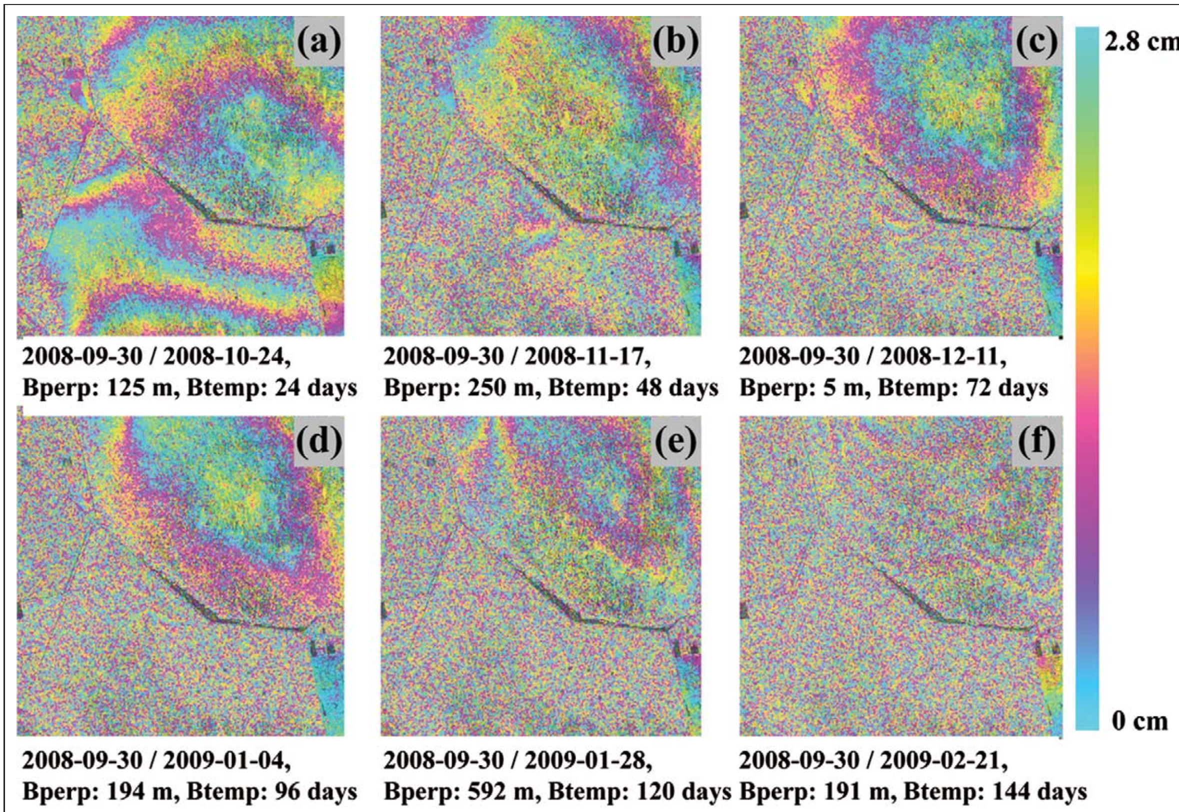

Figure 3. HH polarization interferograms of the northern study area showing coherence degradation with increasing temporal baselines (Btemp). The intensity of the fringes is proportional to the coherence level. Interferograms with relatively shorter temporal baselines ($<$48 days) maintain good coherences in most wetland areas (a, b). Longer time span interferograms (c, d, e, and f) show significant decorrelation over the wetlands. The 144 day interferogram is almost decorrelated over the wetland area (f).

Vol. 37, No. 5, October/octobre 2011

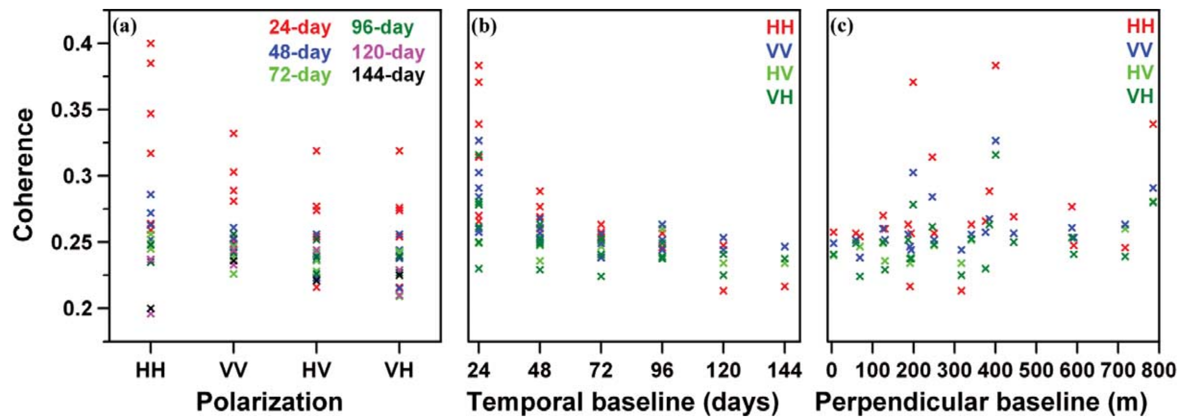

Figure 4. Coherence analysis of the Radarsat-2 quad-polarization interferometric data of northern study area. Co-polarization (HH and VV) interferograms yield higher coherence than cross-polarization (HV and VH), indicating that HH polarization is most suitable for the wetland InSAR application (a). The HV and VH polarization show very similar levels of coherence. The analysis shows a strong coherence dependency on the temporal baseline (b) and no dependency on the geometrical baseline (c).

found in a short and intermediate high mangrove area, which was adjusted to the transition of salt- and fresh-water wetlands. These interferograms reflected water level changes due to ocean tides. The tide-induced fringes were clearly visible in the two 24 day interferograms (23 September 2008 and 17 October 2008 and 17 October 2008 and 10 November 2008) (**Figures 7a** and **7c**). However, the 48 day temporal baseline interferogram did not show much tide-induced signal, probably because the two acquisitions were taken during similar tide conditions (**Figure 7b**). The interferogram was incoherent in the southwest corner, which is characterized by tall mangrove vegetation.

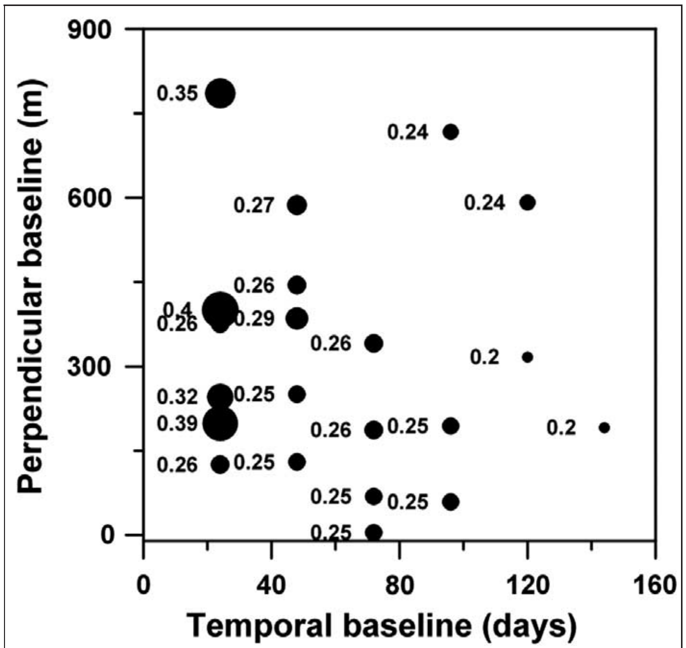

Figure 5. Coherence analysis of all Radarsat-2 HH polarization interferometric pairs. The analysis shows a strong coherence dependency on the temporal baseline and less dependency on the perpendicular one.

The coherence in the southern study area depended on the vegetation type, polarization, and temporal baseline. As indicated before, the tall mangrove area in the southwestern corner did not maintain coherence, even with the short 24 day temporal baseline (**Figures 6** and **7**). Thus, if the radar signal reached the water surface through the vegetation regardless the vegetation types, we detected the coherent phase of the water level changes. The density or the height of the vegetation is a critical parameter for the wetland InSAR application. Average coherence values for the entire study areas were calculated to compare the coherence of the different polarization interferograms. The coherence analysis was conducted with an estimation window of 5 pixels $\times$ 5 pixels (**Figure 8**). The coherence of HH co-polarization interferograms showed the highest values (> 0.35), and the next highest coherence of interferograms was found at the VV co-polarization (**Figure 8a**). The cross-polarization interferograms showed the lowest coherence values. We also identified the inverse proportion between coherence and temporal baseline in the four polarization interferograms (**Figure 8b**). In the comparison of the coherence level with the temporal and geometric perpendicular baselines (**Figure 8b** and **8c**), the wetland InSAR application strongly relies on the temporal decorrelation.

Discussion and conclusions

In this study, we found that the Radarsat-2 C-band observations worked very well for the wetland InSAR application. Good coherent phases were maintained in almost all wetland areas as long as the temporal baseline was shorter than 48 days. We also confirmed that the intermediate wavelength C-band (5.6 cm) SAR observations maintained better coherence than the shorter wavelength X-band (3.1 cm) SAR observations with similar temporal duration. Our previous wetland InSAR study of TerraSAR-X indicated that coherence was significantly degraded with temporal baselines exceeding 33 days (Hong et al., 2010a). Hence, the wetland InSAR application prefers longer wavelength SAR acquisitions, although the X-band observations with short temporal baselines (< 33 days) are also very useful in detecting water level changes.

Double-bounce scattering (Richards et al., 1987) is regarded as the main mechanism of the wetland application

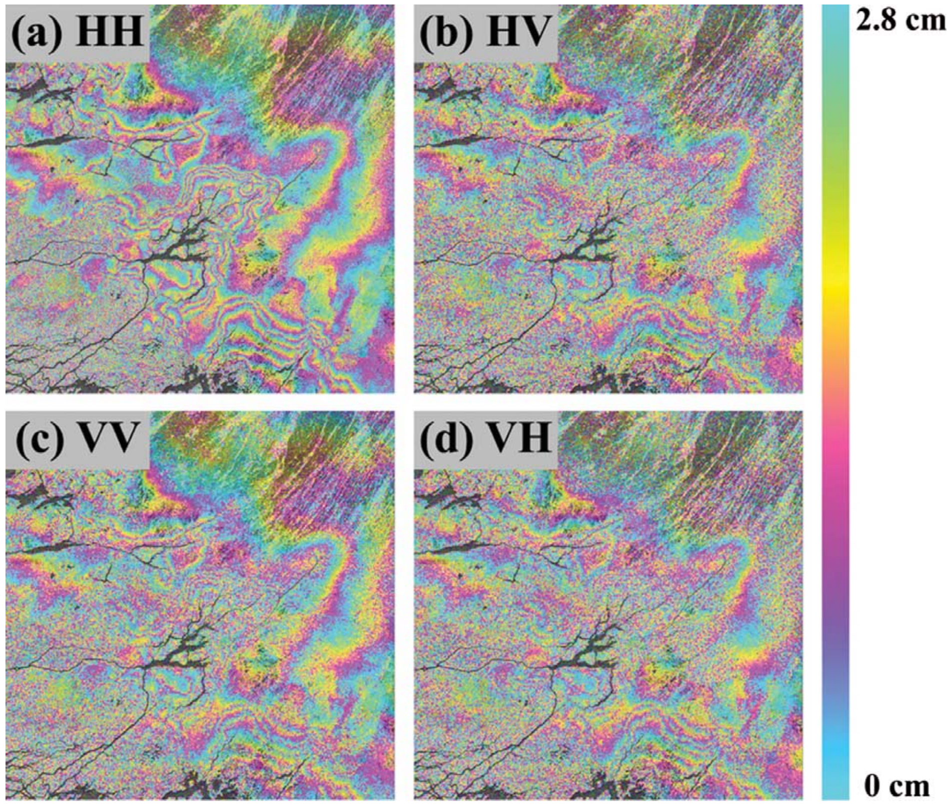

Figure 6. Quad polarimetric interferograms (23 September 2008 and 17 October 2008, Bperp: 415 m, temporal baseline (Btemp): 24 days) of wetlands in southern study area (a–d). Each fringe cycle shows about a 2.8 cm water level change in the line of sight. All of the interferograms show a similar fringe pattern due to water level changes. The long wavelength fringes in the upper right corner are induced by a north–south flow in freshwater herbaceous wetlands. The shorter wavelength fringes in the center of the interferogram reflect water level changes in the saltwater mangroves induced by ocean tides. The decorrelated area in the lower left corner occurs in saltwater marshes covered by tall mangrove.

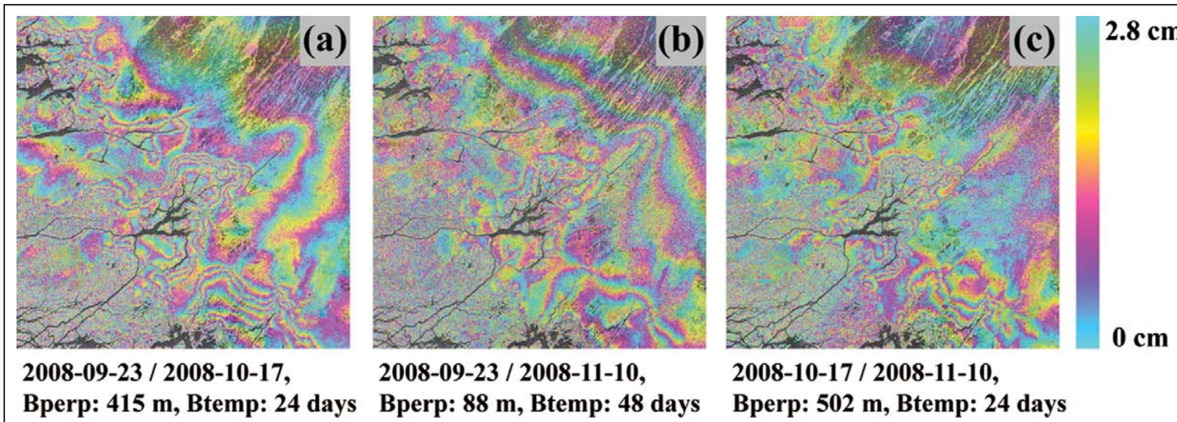

Figure 7. Time series of HH polarization interferograms of the southern study area. The intensity of the fringes is proportional to the coherence level.

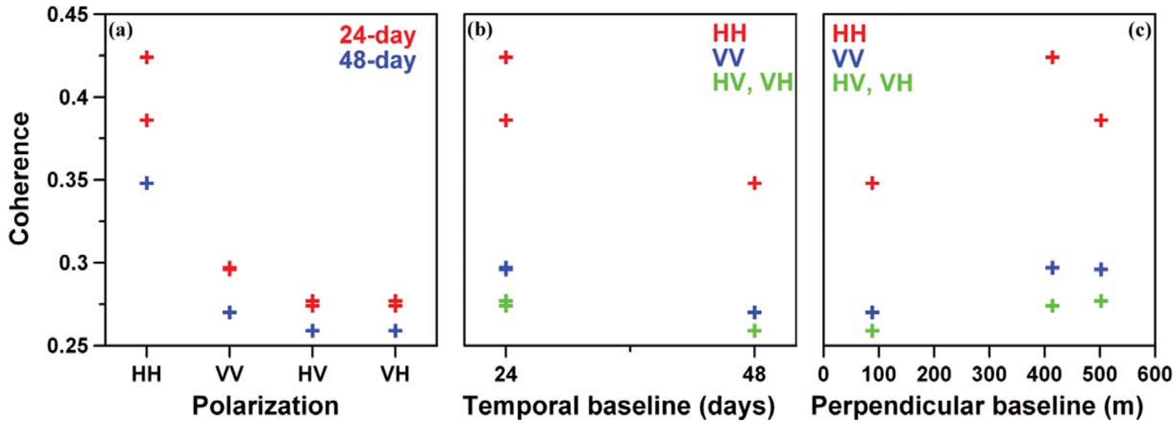

Figure 8. Coherence analysis of the Radarsat-2 quad polarization interferometric data of the southern study area. Co-polarization interferograms (HH and VV) represent significantly higher coherence than the cross-polarization interferogram (HV and VH). Specifically, HH co-polarization shows the highest level of coherence (>0.35) in the natural wetland environment (a). The coherence may be affected by the surface's condition such as vegetation type and density. As shown at the coherence analysis in northern study area, the temporal baseline is a more important factor in maintaining coherence in southern study area compared with geometric perpendicular baseline (b and c).

(Alsdorf et al., 2000; Wdowinski et al., 2004). The quad-polarimetric observations enabled us to make a map of the decomposition into surface-, double-, and volume-scattering mechanisms. We used the simple Pauli decomposition method (Cloude and Pottier, 1996; Boerner et al., 1998; Hellmann, 1999; Karathanassi and Dabboor, 2004) to identify dominant scattering behaviors in this study. The color composite images displayed in **Figures 1c** and **1d** map the three scattering types as follows: blue, surface scattering ($S_{HH} + S_{VV}$); red, double scattering ($S_{HH} - S_{VV}$); and green, volume scattering ($2S_{HV}$). In **Figure 1c**, double-bounce scattering is dominant in WCA-1, while volume scattering is dominant in WCA-2A. Surface scattering was clearly detected in the agricultural area, as expected. In **Figure 1d**, the freshwater wetlands in the northeast corner are characterized by double-bounce scattering, whereas the saltwater mangroves are characterized by single and volume scatterings.

One of the most interesting results of this study found that the four polarization interferograms showed very similar fringe patterns reflecting surface water level changes. This result confirmed our previous dual-polarization study indicating that the dominant scattering mechanism in wetland InSAR application is double- or more-bounce scattering, in which one of the bounces scatters from the water surface (Hong et al., 2010a). Multiple-bounce scattering, which is also called volume scattering, is usually considered as the cross-polarization signal in common scattering theories. Thus, the cross-polarization signal can be decomposed into the double scattering and the pure volume scattering components (Hong et al., 2009; Hong and Wdowinski, 2010c).

Although all quad polarizations can detect water level changes, the co-polarization signals generated better coherent phases than the cross-polarization interferograms. Interferogram coherence was highest in HH, then VV, and lowest in HV or VH. Hence, we suggest that the HH polarization provides the best results in the wetland InSAR application. Interferometric coherence over the wetland areas was significantly degraded by temporal decorrelation, whereas the coherence in urban area was less dependent on the temporal baseline. The impact of the geometrical perpendicular baseline was very minor for monitoring coherent phases of water level changes compared with the effect of the temporal baseline. Thus, we suggest that the temporal decorrelation is the most important factor in the wetland InSAR application. However, we confirmed that longer wavelength data is more useful for the wetland InSAR application than short wavelength data for similar acquisition parameters including a similar interferometric time span (Wdowinski et al., 2008; Hong et al., 2010a; Hong et al., 2010b).

The Radarsat-2 provided various acquisition modes including the quad-polarization capability used in this study. Although we did not test other acquisition modes of Radarsat-2, there is no doubt that it can successfully replace the previous Radarsat-1 with C-band HH-polarization satellite for the wetland InSAR application. Moreover, the C-band signal (5.6 cm), which was less sensitive to atmospheric artifacts than in the X-band application and to ionosphere effects in the L-band application, is useful for the observation of the water level changes or other surface's displacement. Thus, the Radarsat-2 C-band data greatly contributes to scientific research to understand and manage our precious Earth's environment.

Acknowledgements

This work was funded through NASA Cooperative Agreement No. NNX08BA43A (WaterSCAPES: Science of

Coupled Aquatic Processes in Ecosystems from Space) grants. We thank the Canadian Space Agency (CSA) for access to the Radarsat-2 data with The Science and Operational Applications Research (SOAR) project. We also thank CSA and the Japanese Aerospace Exploration Agency (JAXA) for access to Radarsat-1 and JERS-1 data, respectively.

References

Alsdorf, D.E., Melack, J.M., Dunne, T., Mertes, L.A.K., Hess, L.L., and Smith, L.C. 2000. Interferometric radar measurements of water level changes on the Amazon flood plain. *Nature,* Vol. 404, No. 6774, pp. 174–177. doi: 10.1038/35004560.

Boerner, W.M., Mott, H., Luenburg, E., Livingstone, C., Brisco, B., Brown, R.J., and Patterson, J.S. 1998. *Pinciples and Applications of Imaging Radar, Manual of Remote Sensing*. John Wiley & Sons, Inc., ch. 5, New York.

Buckley, S.M., Rossen, P.A., and Persaud, P. 2000. ROI_PAC Documentation-Repeat Orbit Interferometry Package.

Cloude, S.R., and Pottier, E. 1996. A review of target decomposition theorems in radar polarimetry. *IEEE Transactions on Geoscience and Remote Sensing,* Vol. 34, No. 2, pp. 498–518. doi: 10.1109/36.485127.

Freeman, A., and Durden, S.L. 1998. A three-component scattering model for polarimetric SAR data. *IEEE Transactions on Geoscience and Remote Sensing,* Vol. 36, No. 3, pp. 963–973. doi: 10.1109/36.673687.

Goldstein, R.M., and Werner, C.L. 1998. Radar interferogram filtering for geophysical applications. *Geophysical Research Letters,* Vol. 25, No. 21, pp. 4035–4038. doi: 10.1029/1998GL900033.

Gondwe, B.R.N., Hong, S.-H., Wdowinski, S., and Peter, B.-G. 2010. Hydrologic Dynamics of the Groundwater-dependent Sian Ka'aN Wetlands, Mexico, From InSAR and SAR Data. *Wetlands,* Vol. 30, No. 1, pp. 1–13. doi: 10.1007/s13157-009-0016-z.

Hellmann, M. 1999. Classification of full polarimetric SAR data for cartographic application. Technical University of Dresden.

Hong, S.-H., Wdowinski, S., and Kim, S.-W. 2009. Wetland InSAR over the Everglades from space observed polarimetric data *Proceedings of POLinSAR,* Frascati, Italy.

Hong, S.-H., Wdowinski, S., and Kim, S.-W. 2010a. Evaluation of TerraSAR-X observations for wetland InSAR application. *IEEE Transactions on Geoscience and Remote Sensing,* Vol. 48, No. 2, pp. 864–873. doi: 10.1109/TGRS.2009.2026895.

Hong, S.H., Wdowinski, S., Kim, S.W., and Won, J.S. 2010b. Multi-temporal monitoring of wetland water levels in the Florida Everglades using interferometric synthetic aperture radar (InSAR). *Remote Sensing of Environment,* Vol. 114, No. 11, pp. 2436–2447. doi: 10.1016/j.rse.2010.05.019.

Hong, S.-H., and Wdowinski, S. 2010c. Rotated Dihedral And Volume Scattering Behavior In Cross-Polarimetric SAR. *IGARSS 2010:* Hawaii, U.S.A.

Karathanassi, V., and Dabboor, M. 2004. Land cover classification using ESAR polarimetric data. *Proceedings of XXth ISPRS Congress Commission VII, Istanbul, Turkey,* pp. 280–285.

Lu, Z., and Kwoun, O.I. 2008. Radarsat-1 and ERS InSAR analysis over southeastern coastal Louisiana: Implications for mapping water-level changes beneath swamp forests. *IEEE Transactions on Geoscience and Remote Sensing,* Vol. 46, No. 8, pp. 2167–2184. doi: 10.1109/TGRS.2008.917271.

Wdowinski, S., Amelung, F., Miralles-Wilhelm, F., Dixon, T.H., and Carande, R. 2004. Space-based measurements of sheet-flow characteristics in the Everglades wetland, Florida. *Geophysical Research Letters,* Vol. 31, No. 15. doi: 10.1029/2004GL020383.

Wdowinski, S., S.-W., K., Amelung, F., and Dixon, T. 2006. Wetland InSAR: A new spacebased hydrological monitoring tool of wetlands surface water level changes. *GlobWetland Symposium proceedings.*

Wdowinski, S., Kim, S.W., Amelung, F., Dixon, T.H., Miralles-Wilhelm, F., and Sonenshein, R. 2008. Space-based detection of wetlands' surface water level changes from L-band SAR interferometry. *Remote Sensing of Environment,* Vol. 112, No. 3, pp. 681–696. doi: 10.1016/j.rse.2007.06.008.

Yamaguchi, Y., Moriyama, T., Ishido, M., and Yamada, H. 2005. Four-component scattering model for polarimetric SAR image decomposition. *IEEE Transactions on Geoscience and Remote Sensing,* Vol. 43, No. 8, pp. 1699–1706. doi: 10.1109/TGRS.2005.852084.